

Glimpses of Violation of Strong Cosmic Censorship in Rotating Black Holes

Marc Casals^{1,2} and Cássio I. S. Marinho¹

¹*Centro Brasileiro de Pesquisas Físicas (CBPF), Rio de Janeiro, CEP 22290-180, Brazil.*

²*School of Mathematics and Statistics, University College Dublin, Belfield, Dublin 4, Ireland.*

Rotating and/or charged black hole spacetimes possess a Cauchy horizon, beyond which Einstein's equations of General Relativity cease to be deterministic. This led to the formulation of the Strong Cosmic Censorship conjecture that such horizons are unstable. We consider linear field perturbations of rotating and electrically-charged (Kerr-Newman-de Sitter) black holes in a Universe with a positive cosmological constant. By calculating the quasinormal modes for scalar and fermion fields, we provide evidence for the existence of weak solutions to Einstein's equations across the Cauchy horizon in the nearly-extremal regime. We thus provide evidence for violation of Strong Cosmic Censorship in these rotating black hole spacetimes.

I. INTRODUCTION

Black holes are exact solutions of Einstein's equations of General Relativity. When a black hole is rotating and/or is electrically charged, there is a null hypersurface in its inside, called the Cauchy horizon, beyond which the Cauchy value problem is not well-posed: Einstein's equations cease to be deterministic. However, black holes in Nature form from the gravitational collapse of matter and they are not in isolation. It is therefore important to ascertain whether the Cauchy horizon is stable under matter field perturbations.

Penrose's strong Cosmic Censorship (SCC) [1] essentially conjectures that the Cauchy horizons are unstable, so that Einstein's equations are deterministic inside – as well as outside – the black holes that exist in Nature. More specifically, Christodoulou's formulation of SCC [2] conjectures that Einstein equations do not admit *weak* solutions (i.e., metric solutions with a locally square integrable derivative) across a Cauchy horizon formed from generic initial data. Given the notorious difficulty in solving Einstein's nonlinear and coupled equations, it is useful and common to, instead, analyze the equations of *linear* field perturbations which, in their turn, source higher order metric perturbations. The linear perturbations can be gravitational or some matter field's – either as an analogue of the linear gravitational perturbations or of physical interest in their own right.

It has been shown that SCC, whether in its nonlinear or linear version, is respected for non-rotating and charged (Reissner-Nordström) black holes [3–7], as well as rotating and neutral (Kerr) black holes [8–10]. Within the linear perturbation setup, this is essentially due to the fact that the perturbation, even though it decays outside the black hole, it does not do so fast enough to compensate for the blueshift that it experiences as it approaches the Cauchy horizon. This leads to the field energy of the field blowing up at the Cauchy horizon. That is the case for all the asymptotically flat black holes mentioned above [60], i.e., black holes in a Universe with zero cosmological constant, $\Lambda = 0$. However, the existence of

a positive cosmological constant $\Lambda > 0$ in the Universe, i.e., a de Sitter (dS) Universe, may “disperse” the field perturbation enough so that when it reaches the Cauchy horizon it is not strong enough to destabilize it. We will therefore only consider black holes in a dS Universe from now on.

A way of measuring the “strength” of a linear field perturbation outside a black hole is via the so-called quasinormal modes (QNMs; see, e.g., [11, 12] for reviews). These are field modes with a complex frequency ω_{QN} , whose imaginary part determines the decay rate of the mode outside the black hole. Indeed, a key quantity is $\beta \equiv -\text{Im}(\omega_{QN})/\kappa_-$ for the slowest-decaying QNM, where κ_- is the surface gravity of the Cauchy horizon. It has been shown [13–19] that, for Reissner-Nordström-dS (RNdS) and Kerr-dS black holes, $\beta > 1/2$ corresponds to the linear perturbations being locally square integrable at the Cauchy horizon and so to violation of Christodoulou's SCC. Furthermore, $\beta > 1$ indicates regularity of the curvature invariants on the Cauchy horizon when including gravitational backreaction. Indeed, nonlinear results (e.g., [20–23]) suggest that conclusions about SCC drawn at the linear level carry over to the nonlinear level.

In the case of RNdS, it has been recently shown that $\beta > 1/2$, and even $\beta > 1$ [61], are possible in the nearly-maximal charge regime (i.e., for a near-extremal RNdS black hole) when considering various types of linear perturbations: massless or massive, charged or neutral, scalar [17, 24–27] (see also [28]), neutrino [16, 18] or gravitoelectromagnetic [15] fields. Still within spherical symmetry but in the *nonlinear* setup, SCC violation has been found near extremality by evolving initial data for a massless or massive, neutral scalar field minimally coupled to the Einstein-Maxwell system in dS [23]. We note that the recent work in [29], however, claims that SCC is preserved in that setting when adding charge to the massless scalar field.

It is, however, expected that all black holes in Nature are rotating (e.g. [30]) and so it is particularly important to investigate whether the Cauchy horizons of *rotating* black holes are stable. So far, all investigations for rotating black holes were in the linear scenario and

they all found that SCC is preserved ($\beta < 1/2$). That was shown in [14] for massless neutral and minimally-coupled scalar perturbations as well as for gravitational perturbations of Kerr-dS (see also App.B). In charged Kerr-dS (i.e., Kerr-Newman-dS, KNdS), SCC preservation was observed in [31] for massless neutral fields, where only angular momentum a above a certain critical value was considered, and in [32], where only a limited range of parameters was investigated.

In this work we show that violation of SCC can actually be achieved in KNdS black holes. Specifically, we calculate the QNMs of massless, both neutral and charged, (conformally-coupled) scalar and fermion linear field perturbations of KNdS. We then show that $\beta > 1/2$ (if only considering fields with small charge, even $\beta > 1$) is possible in the near extremal and non-highly-rotating regime.

II. PERTURBATIONS OF KNdS BLACK HOLES

The line-element of KNdS black holes with mass M , angular momentum per unit mass a and charge Q can be written, in units $c = G = 1$, as [33, 34]

$$ds^2 = -\frac{\Delta_r}{\rho^2 \Xi^2} (dt - a \sin^2 \theta d\varphi)^2 + \frac{\Delta_\theta \sin^2 \theta}{\rho^2 \Xi^2} (a dt - (r^2 + a^2) d\varphi)^2 + \rho^2 \left(\frac{d\theta^2}{\Delta_\theta} + \frac{dr^2}{\Delta_r} \right), \quad (1)$$

where $t, r \in \mathbb{R}$, $\theta \in [0, \pi]$, $\varphi \in [0, 2\pi]$,

$$\rho^2 \equiv r^2 + a^2 \cos^2 \theta, \quad \Delta_\theta \equiv 1 + \alpha \cos^2 \theta, \quad (2)$$

$$\Delta_r \equiv (r^2 + a^2) \left(1 - \frac{r^2}{L^2} \right) - 2Mr + Q^2, \quad (3)$$

$\alpha \equiv \Xi - 1 \equiv a^2/L^2$ and $L \equiv \sqrt{3/\Lambda}$. The radial function Δ_r has four roots: the radii of the event horizon r_+ , of the Cauchy horizon r_- , of the Cosmological horizon r_c and a negative root r_{--} ; they satisfy $r_{--} < 0 < r_- \leq r_+ < r_c$. Each horizon $j \in \{+, -, c\}$ has an associated angular velocity $\Omega_j = a/(r_j^2 + a^2)$, surface gravity $\kappa_j = |\Delta'_r(r_j)|/(2\Xi(r_j^2 + a^2))$ (such that $\kappa_+ \leq \kappa_-$) and electric potential $\phi_j \equiv \phi(r_j)$, where $\phi(r) \equiv Qr/(\Xi(r^2 + a^2))$. Extremal black holes correspond to $r_- = r_+$, which is achieved at the upper bounds $Q = Q_{max}$ and $a = a_{max}$ for charge and rotation. In the extremal limit, it is $\kappa_+ \sim \kappa_- \rightarrow 0^+$.

We consider linear perturbations of KNdS by a massless field of charge q and spin s , with $s = 0$ for a scalar field with conformal coupling parameter $\xi = 1/6$ and $s = \pm 1/2$ [62] for a fermion field [63]. The equations obeyed by these perturbations separate by variables (and

decouple for $s = \pm 1/2$). The field perturbations thus admit a decomposition into modes, for which the time and azimuthal-angle dependence is $e^{-i\omega t + im\varphi}$, where $\omega \in \mathbb{C}$ is the mode frequency and $m \in \mathbb{Z}$. The radial and angular factors obey the following ordinary differential equations, respectively [35]:

$$\left[\Delta_r^{-s} \partial_r \Delta_r^{s+1} \partial_r + \frac{W^2 - isW\Delta'_r}{\Delta_r} + 2isW' - Y \right] R(r) = 0, \quad (4)$$

$$\left[\partial_u \Delta_u \partial_u - \frac{1}{\Delta_u} \left(H + \frac{s}{2} \Delta'_u \right)^2 + 2sH' - X \right] S(u) = 0, \quad (5)$$

where

$$W \equiv \Xi[\omega(r^2 + a^2) - am] - qQr, \\ Y \equiv \frac{2}{L^2}(s+1)(2s+1)r^2 + {}_s\lambda_{\ell m}. \quad (6)$$

and

$$H \equiv \Xi[a\omega(1 - u^2) - m], \quad \Delta_u \equiv (1 - u^2)(1 + \alpha u^2), \\ X \equiv 2(2s^2 + 1)\alpha u^2 - {}_s\lambda_{\ell m} + s(1 - \alpha), \quad u \equiv \cos \theta. \quad (7)$$

The primes in Δ'_r and W' denote derivatives with respect to r and in Δ'_u and H' with respect to u . Here, ${}_s\lambda_{\ell m} = {}_s\lambda_{\ell m}(\omega)$ is the angular eigenvalue, where $|m| \leq \ell = |s|, |s|+1, |s|+2, \dots$ is a multipolar index that labels the eigenvalues.

QNMs correspond to frequencies $\omega = \omega_{QN}$ such that the radial solution is purely ingoing into the event horizon and purely outgoing to the cosmological horizon, i.e., neglecting constant factors,

$$\Delta_r^s R \sim e^{-i\omega r_*}, \quad r \rightarrow r_+^+, \\ R \sim e^{+i\omega_c r_*}, \quad r \rightarrow r_c^-, \quad (8)$$

where r_* is defined via $dr_* = \Xi(r^2 + a^2)dr/\Delta_r$ and $\omega_j \equiv \omega_{QN} - m\Omega_j - q\phi_j$, with $j \in \{+, c\}$. The QNM condition effectively turns the radial Eq. (4) into an eigenvalue problem similar to that of the angular Eq. (5). For each ℓ and m there exists an infinite number of QNMs, labelled by the so-called overtone index $n = 0, 1, 2, \dots$ for increasing values of $-\text{Im}(\omega_{QN})$; the ‘‘fundamental’’ $n = 0$ being the slowest-decaying overtone.

III. QNM FAMILIES

The QNMs of black holes in dS, including KNdS, can be broadly divided into three families: the photon-sphere (PS), the near-extremal (NE) and the de Sitter (dS) modes.

The PS modes are associated with the unstable spherical photon orbits of the spacetime. The eikonal approximation (i.e., large- ℓ) yields an expression for the

PS modes in terms of properties of the photon orbits [14, 32, 36–40]. We have numerically checked that the slowest-decaying PS mode in KNdS is the one with $\ell = m$, which corresponds to the co-rotating equatorial photon orbit. We derived [41] the eikonal approximation for the PS frequencies for $\ell = m$ for a neutral field (the s -dependence only comes in at higher-order terms for large- ℓ [39]) in KNdS space-time and we obtained

$$\omega_{\text{PS}} \equiv \zeta \Omega_{\text{ph}} - i \left(n + \frac{1}{2} \right) \lambda. \quad (9)$$

Here, Ω_{ph} and λ are, respectively, the angular velocity and the Lyapunov exponent (i.e., the inverse of the instability timescale) of the (unstable) co-rotating circular photon orbit at a radius $r = r_{\text{ph}}$ on the equatorial plane; their expressions are given in App.C. We have checked numerically that $\zeta = \ell + 1/2$ works well for small a/M and $\zeta = m$ for large a/M (see Sec.IV.B [42] in Kerr). The imaginary part in Eq. (9) for $n = 0$ agrees very well with our numerical results across all a/M . We have numerically observed that, when considering the field to have a charge q , a better approximation to the real part of the PS modes is that in (9) plus $q\phi(r_{\text{ph}})$.

In their turn, the NE frequencies are obtained by carrying out near-extremal asymptotics and assuming that their imaginary part goes to zero in that limit (e.g., [43] in Reissner-Nordström, [42, 44] in Kerr and [24, 26] in RNdS). We carried out a similar near-extremal asymptotic analysis in KNdS and we obtained [41]:

$$\omega_{\text{NE}} \equiv m\Omega_+ + q\phi_+ + \kappa_+ \left(m\bar{\Omega} + q\bar{\phi} - i\kappa_+ \left(n + \frac{1}{2} + \sqrt{(s+1/2)^2 + \bar{\lambda} - (m\bar{\Omega} + q\bar{\phi})^2} \right) \right), \quad (10)$$

where $\bar{\Omega} \equiv \frac{\Omega_- - \Omega_+}{2\kappa_+} \Big|_{r_+ \rightarrow r_-}$, $\bar{\phi} \equiv \frac{\phi_- - \phi_+}{2\kappa_+} \Big|_{r_+ \rightarrow r_-}$ and

$$\bar{\lambda} \equiv \frac{L^2 {}_s\lambda_{\ell m} (m\Omega_+ + q\phi_+) + 2r_+^2 (1+s)(1+2s)}{(r_c - r_+)(r_c + 3r_+)} \Big|_{r_- \rightarrow r_+}. \quad (11)$$

We note that Eq. (10) was obtained using the right QNM boundary condition at r_+ but an *ad hoc* boundary condition away from r_+ so that it is an approximation to the NE frequencies that works better the closer r_c is to r_+ [64].

Finally, the dS modes are associated with KNdS space-time with $M = Q = 0$ (i.e., vacuum and event horizon-less). We see numerically that the dS frequencies are well approximated by

$$\omega_{\text{dS}} \equiv m\Omega_{c,0} - i(\ell + n + 1)\kappa_{c,0}, \quad (12)$$

where $\Omega_{c,0} \equiv \frac{a}{a^2 + L^2}$ and $\kappa_{c,0} \equiv \frac{L}{a^2 + L^2}$ are, respectively, the angular velocity and surface gravity of the cosmological horizon $r = r_c$ for $M = Q = 0$. This approximation

in KNdS was motivated by the QNMs in pure de Sitter spacetime [45] and by the corresponding expressions in RNdS [16, 24]. Eq. (12) is for neutral fields, for large q we observed numerically that the real part goes to that in (12) plus $q\phi_c|_{M=Q=0}$.

We now discuss the dominance at late times of the various mode families in the case of neutral fields and in the near-extremal black hole regime. Importantly, there exists a critical value \bar{a} such that for $a < \bar{a}$ the square root in Eq. (10) is real for any ℓ and m . On the other hand, for $a > \bar{a}$, the square root becomes complex for some large enough value of m . Furthermore, we have checked that, as $r_+ \rightarrow r_-$, $\lambda \sim \kappa_+ \rightarrow 0$ if $a \gtrsim \bar{a}$ whereas λ goes to a nonzero value if $a \lesssim \bar{a}$ [65]. Consequently, for $a \gtrsim \bar{a}$, $\text{Im}(\omega_{\text{PS}})$ goes to zero and β_{PS} goes to a nonzero finite value; we have checked that, in this case, the PS family is the dominant one. On the other hand, for $a \lesssim \bar{a}$, $\text{Im}(\omega_{\text{PS}})$ does not go to zero and the NE family is the dominant one. With regards to the dS modes, the slowest-decaying ones in the approximation (12) are clearly those with $n = 0$ and the smallest multipole number: $\ell = |s|$. We have numerically checked that, indeed, the slowest-decaying dS modes are those with $\ell = m = |s| = 0, 1/2$, and that is also true for the NE modes.

Let us now turn on the field charge. The symmetries of the QNM eigenvalue problem (namely, Eqs. (4), (5) and (8)) imply that, under $\{m, q\} \rightarrow \{-m, -q\}$, we have $\omega_{QN} \rightarrow -\omega_{QN}^*$. Thus, consider, in particular, the $m = 0$ modes: for $q = 0$ they lie symmetrically with respect to the negative imaginary axis, but that symmetry is broken as $|q|$ increases. Indeed, this leads to two different behaviours in the PS modes as $|q|$ increases, depending on whether the real part of the frequencies for $q = 0$ is positive or negative. The $m = 0$ dS and NE modes, as opposed to any other modes, lie on the imaginary axis for $q = 0$ and, as $|q|$ increases, they move away from it singly (i.e., without splitting into modes with different behaviours).

A particularly important limit is that of large field charge. We have carried out a WKB analysis in that limit for the charged, (conformally-coupled) scalar and fermion fields in KNdS, similar to the analyses in [18, 26] in RNdS. Our large- q WKB expression for the QNM frequencies ω_j , with $j \in \{+, c\}$, is

$$\omega_{j,q} \equiv s_j \frac{\kappa_j (r_j^2 + a^2)}{2Q(r_j^2 - a^2)} \lambda_q - \frac{i}{2} \kappa_j + O\left(\frac{1}{qr_c}\right), \quad (13)$$

corresponding to a “black hole family” ($j = +$) and a “cosmological family” ($j = c$). Here, $s_+ \equiv +1$, $s_c \equiv -1$ and λ_q is the coefficient in the leading-order eigenvalue asymptotics for large q : ${}_s\lambda_{\ell m} = \lambda_q q + O(1)$, which results from ${}_s\lambda_{\ell m} = O(\omega) = O(q)$ (e.g., [46] in Kerr). These two WKB families are the limiting values for the two different behaviours in the PS modes mentioned above

when the symmetry is broken as q increases from zero. Also, the NE modes asymptote to $\omega_{+,q}$ for large- q (as can be checked by comparing (10) for large- q with (13) for $j = +$ in the near-extremal limit).

IV. RESULTS FOR COSMIC CENSORSHIP

The actual value of β for a field perturbation in KNdS is equal to $\min\{\beta_{\text{PS}}, \beta_{\text{NE}}, \beta_{\text{dS}}\}$, where $\beta_{\text{PS/NE/dS}}$ denotes the “exact” value of β for the PS/NE/dS family of modes. We briefly describe in App.A the method that we used for calculating the exact QNM frequencies and $\beta_{\text{PS/NE/dS}}$. The relationship described in the Introduction between the regularity of the of the Cauchy horizon and the values $\beta = 1/2$ and 1 continues to hold (for the ingoing part of the Cauchy horizon) in our setup in KNdS, since we have extended [41] to our $s = 0, 1/2$ fields in KNdS the analyses in [15, 19]. We next present our results for β and SCC, first considering neutral fields and later charged fields.

Fig.1 shows contour plots of β for the neutral spin-0 and spin-1/2 fields as a function of angular momentum a and black hole charge Q (near Q_{max}) for fixed cosmological constant Λ . It also shows the regions where each PS, NE and dS family dominates. Fig.1 clearly shows that there exist regions of parameter space where $\beta > 1/2$, including subregions where $\beta > 1$ for both spin-0 and spin-1/2 fields. Generally, the closer Q is to Q_{max} for fixed a/M , the larger the β ; when increasing a/M for fixed Q , β decreases until reaching a minimum and then it increases (while not surpassing $\beta = 1/2$). The region of largest β , within the parameter ranges included, is for Q closest to Q_{max} , as expected, and smallest a/M . With regards to the dominance of the three families of modes, for $s = 0$ the NE family dominates in the region of smaller rotation and larger charge; the dS family in the region of smaller both rotation and charge; and the PS family in the rest of the range in the plot. For $s = 1/2$ it is similar to $s = 0$ except that the PS family also dominates in the region of smaller both rotation and charge. Finally, we note that we consistently found $\beta < 1/2$ for spacetime parameter values outside the ranges in Fig.1.

We now wish to see the effects as we turn on the field charge q . It follows from Eq. (13) that the β values for the two large- q WKB families $j \in \{+, c\}$ asymptote to $\beta_j \equiv \kappa_j/(2\kappa_-)$. Since $\beta_c \rightarrow \infty$ and $\beta_+ \rightarrow (1/2)^-$ in the extremal limit, the relevant scenario for SCC in the large q regime is the black hole WKB family near extremality. Furthermore, since $\beta_+ \leq 1/2$, in principle, β should not be larger than $1/2$ for large q . However, the WKB analysis leading to (13) has ignored non-perturbative terms and so we proceed to show results of our “exact” numerical investigation. The top plot in Fig.2 shows the imaginary part of the most dominant QNM frequencies as a function of q for $s = 0$ near extremality. The be-

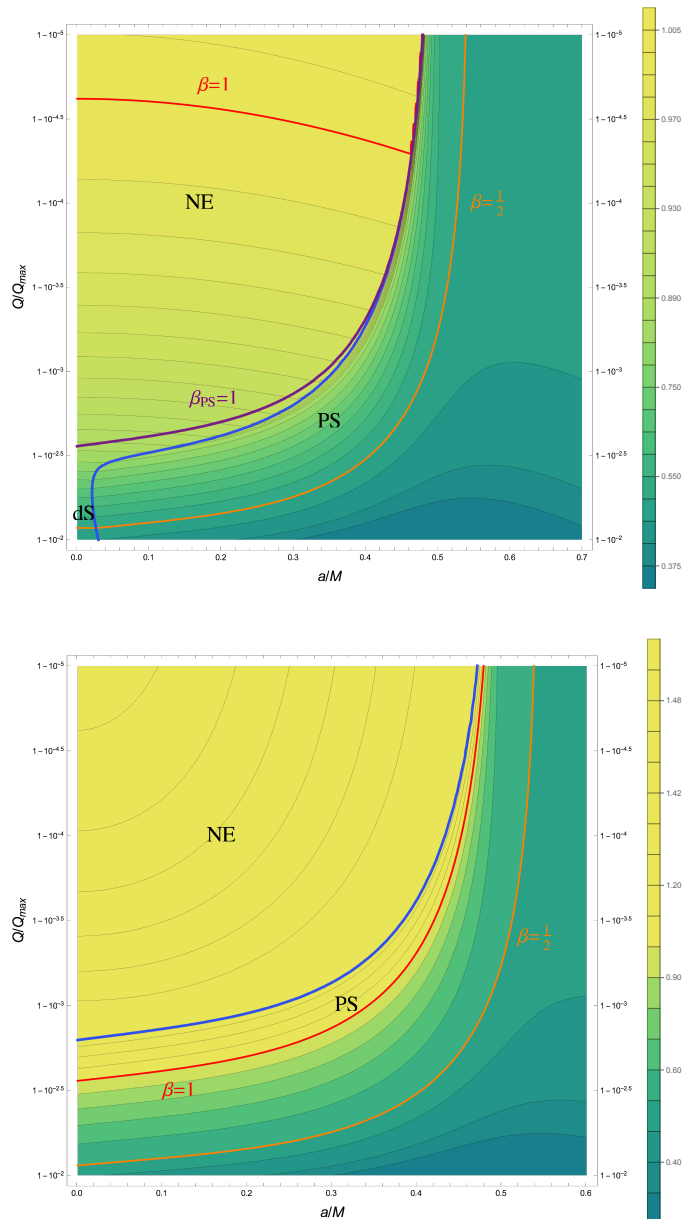


Figure 1: Contour plots of β as a function of a/M (on a linear scale) and Q/Q_{max} (on a log-scale) for $q = 0$, $\Lambda M^2 = 0.02$; field spin $s = 0$ (top) and $s = 1/2$ (bottom). The red and orange curves correspond to, respectively, $\beta = 1$ and $\beta = 1/2$. For reference, we include in the $s = 0$ case, the purple curve corresponding to $\beta_{\text{PS}} = 1$. The blue curves separate the regions of dominance of the PS, NE and dS families (in the $s = 0$ case, the curve separating the regions of NE and dS dominance is not drawn since there is a mode swapping [41], but it roughly corresponds to the continuation to $a = 0$ of the blue line before it drops; in the $s = 1/2$ case, the dS family is not dominant anywhere in the region considered).

haviour of the PS modes as q increases is rather distinct in two regimes. For $a \lesssim \bar{a}$, β_{PS} is well above $1/2$ at least over a significantly large q region and so the NE domi-

nate there. For $a \gtrsim \bar{a}$, on the other hand, β_{PS} rapidly approaches (seemingly monotonically – see the inset) the asymptotic value $\beta_+ \leq 1/2$, thus preserving SCC. Let us now turn to the NE modes. As q increases from zero, β_{NE} decreases until (approximately) the square root in Eq. (10) becomes purely imaginary – let us denote by $q = \bar{q}$ that critical value. Then, for $q > \bar{q}$, β_{NE} displays “wiggles” around the asymptotic value β_+ . These wiggles are a non-perturbative effect missed by the WKB analysis and their amplitude decreases rapidly with q . As a consequence, the severe SCC violation with $\beta > 1$ observed for $q = 0$ is foiled for large q . On the other hand, the presence of the wiggles means that, for $a \lesssim \bar{a}$ and a given arbitrarily large value of q (or at least over the significantly large q region where $\beta_{PS} > 1/2$), one can find interval(s) of values of Q close enough to Q_{\max} in which $\beta > 1/2$ [66]. As is clear from the plot, however, as q increases, one would need more and more (ℓ, m) NE modes to synchronize their wiggles so that $\beta > 1/2$ can be achieved. The bottom plot of Fig.2 is like the top plot but for $s = 1/2$ instead. Its features are essentially the same as for $s = 0$ except for the notable difference that, whereas β_{NE} for $s = 0$ increases with rotation (for fixed q) before the wiggles, it instead decreases for $s = 1/2$. Accordingly, whereas the wiggles start at a larger value of q as rotation increases for $s = 0$, they instead start at a smaller value of q for $s = 1/2$. Thus, increasing rotation within $a \lesssim \bar{a}$ helps achieve SCC violation $\beta > 1/2$ for $s = 0$ whereas it hinders violation for $s = 1/2$. In terms of the specific (ℓ, m) modes, it is worth noting that, whereas $m = \ell = |s| = 0, 1/2$ is the dominant NE mode before the wiggles, that is no longer the case in the wiggling region as higher ℓ 's (and $m \neq \ell$, as is clear in the bottom plot) start wiggling at larger values of q so that they may become the dominant NE modes for some intervals there.

Last but not least, Fig.3 shows that wiggles also appear in β as a function of $1 - r_-/r_+$ [67]. As may be inferred from Fig.2, the amplitude of the wiggles here increases with rotation for $s = 0$ but decreases for $s = 1/2$. Since $\beta_+ \rightarrow 1/2$ in the extremal limit, for $a \lesssim \bar{a}$ and a given field charge $q > \bar{q}$, one can in principle find black holes sufficiently close to extremality which have a $\beta > 1/2$, thus violating SCC. Fig.3 provides examples of regions of (rotating and non-rotating) black hole parameter space where violation occurs when including both $s = 0$ and $s = 1/2$ charged fields. Every time the wiggles go above $1/2$, we catch a glimpse of SCC violation which, as we discussed for Fig.2, fades away as q increases.

V. DISCUSSION

We have calculated the various families of QNMs for neutral and charged, scalar and fermion field perturbations of KNdS black holes. We have shown that there exist regions of phase space $\{M, a, Q, \Lambda\}$ where $\beta > 1/2$

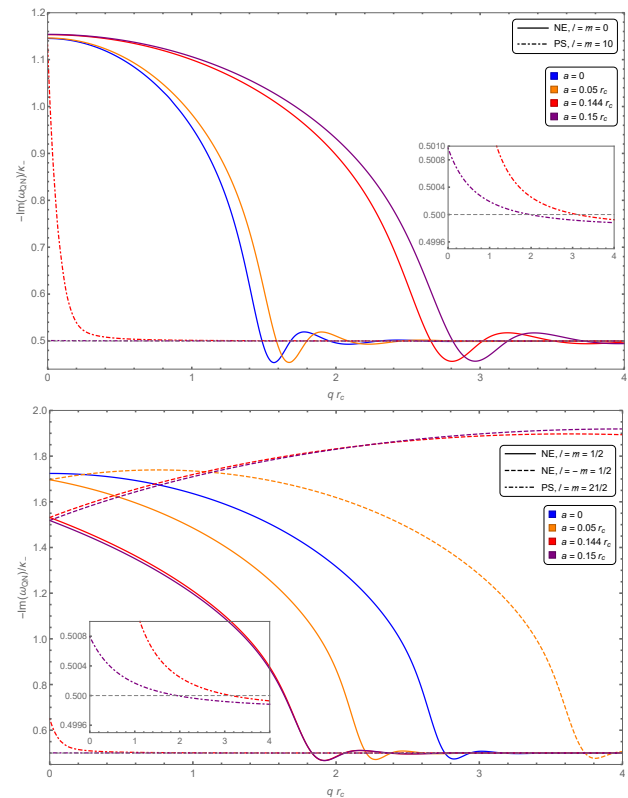


Figure 2: Plots of $-\text{Im}(\omega_{QN})/\kappa_-$ for the most dominant modes as a function of qr_c for $r_+ = r_c/3$, $Q = (1 - 10^{-4}) Q_{\max}$ for various values of a and for $s = 0$ (top) and $s = 1/2$ (bottom). For reference, here it is $\bar{a} \approx 0.135r_c$ and, in units of M , the spacetime parameter values are $Q/M \approx 0.897$, $a/M \approx 0.512$ and $\Lambda M^2 \approx 0.1273$ in the case $a = 0.15r_c$. The values for the PS family and those for the PS family not shown are larger than the ranges included in the plots. The (ℓ, m) values of the modes used for each family is indicated in the labels (for PS, a higher $\ell = m > 10$ is more dominant but the pattern of fast decay to $1/2$ continues to hold); the insets zoom in on the PS family for small qr_c .

for both scalar and fermion fields, signaling the existence of weak solutions across the Cauchy horizon (and, if only considering neutral fields, even $\beta > 1$, signaling regularity of the curvature at the Cauchy horizon). To the best of our knowledge, this is the first time that evidence for violation of SCC has been provided for a (4-dimensional) *rotating* black hole.

Regarding the parameter space considered, we have included black hole rotation and nonzero cosmological constant, which are important for modelling black holes in Nature and the accelerated expansion of the Universe [47, 48]. However, the large values of black hole charge required for SCC violation are astrophysically unrealistic [49]. As for the matter fields, considering them to be charged is required for the formation of a charged black hole. Again, physically realistic values correspond to $qr_c \gg 1$, where the glimpses of SCC violation fade

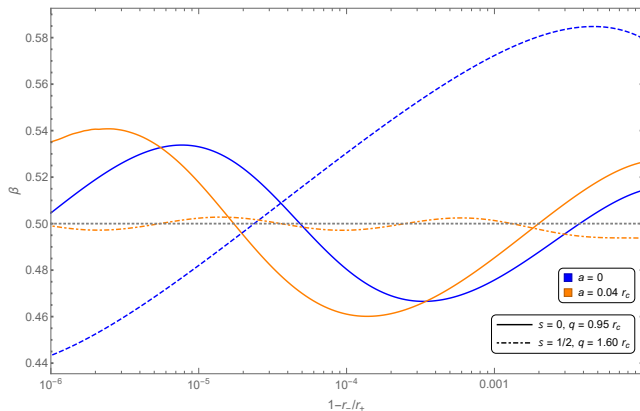


Figure 3: Plot of β as a function of $1 - r_-/r_+$ for $r_+ = r_c/2$ for the cases: (i) $s = 0$ and $q = 0.95r_c$ (continuous), and (ii) $s = 1/2$ and $q = 1.6r_c$ (dotdashed), both for $a = 0$ (blue) and $a = 0.04r_c$ (orange). The critical value $\beta = 1/2$ is indicated as a horizontal dotted black line.

away. However, at least from a fundamental perspective, the SCC violation that we have shown remains disturbing. From that perspective, two different options proposed recently are probably worth investigating further: the inclusion of non-smooth initial data [50] or of quantum effects (e.g., [51] in RNdS).

VI. ACKNOWLEDGEMENTS

Both MC and CM acknowledge partial financial support by CNPq (Brazil), process number 310200/2017-2 in the case of MC.

Appendix A: Numerical method

In order to obtain the exact QNM frequencies, we extended to KNdS the method that Leaver [52] originally developed and applied to Kerr spacetime and was later extended to Kerr-dS in Ref. [53]. Essentially, the method consists of expanding the angular solution $S(u)$ about one endpoint $u = \pm 1$ and then requiring regularity at the other endpoint, which leads to a continued fraction equation for ${}_s\lambda_{\ell m}(\omega)$. Similarly, expanding the radial solution $R(r)$ about the cosmological horizon $r = r_c$ and requiring the QNM boundary condition (8) leads to a continued fraction equation (which involves ${}_s\lambda_{\ell m}$) for the frequency. We then numerically solve the coupled set of the two continued fraction equations.

Our numerical method for obtaining QNM frequencies requires initial seeds, for which we used a combination of the analytic expressions in Eqs. (9), (10) and (12) together with frequencies that we numerically calculated previously at slightly different values of black hole and field parameters.

As a first check of our method, we found, in KNdS, agreement to all digits with the QNMs in tables in [54] for $|s| = 1/2$ as well as visual agreement with Fig.3 [55] (see App.B for agreement in Kerr-dS). We shall give full details of the method in [41].

Appendix B: QNMs and SCC in Kerr-de Sitter

We also ran our code in Kerr-de Sitter (i.e., $Q = 0$) with two objectives. First, as a further check of our code: we checked that, for $s = -2$, we found agreement to all digits with the QNMs in tables in [53] as well as visual agreement with their plots.

The second objective is to investigate the claim in [56] that, in Kerr-dS, $\beta > 1/2$ is possible for $s = 1/2$. In Fig.4 we plot the imaginary part of the most dominant QNM frequencies for spin-1/2 as a function of a/a_{\max} in the case of Fig.2 (top left) in [56], where [56] claims violation of SCC. Our curves for the dS modes for $\ell = 1/2$ and $\ell = 3/2$ agree with the curves in [56] (after the curve for $\ell = 1/2$ crosses $\beta = 1/2$, though, there is a swapping of modes [41] and the difference between our curve and the one in [56] is just a matter of family labelling – in any case, this is irrelevant for SCC). However, our Fig.4 shows that, while the slowest decaying mode for $\ell = 1/2$ is indeed a dS mode, the slowest decaying mode for $\ell = 3/2$ is instead a PS mode. It seems that this mode is missed by [56] and, since it has $-\text{Im}(\omega_{QN})/\kappa_- < 1/2$, it is in fact crucial for saving SCC. We have carried out similar comparisons for other values of black hole parameters (including the region in Fig.2 (top right) in [56] where violation is claimed) and find the same outcome: Ref. [56] seems to follow the dS family only and others modes save SCC where [56] claims violation.

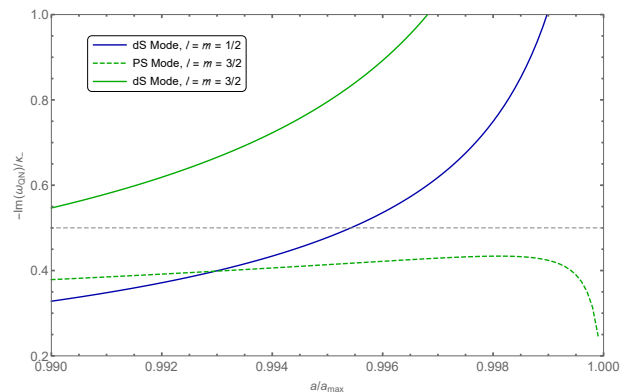


Figure 4: Plot of $-\text{Im}(\omega_{QN})/\kappa_-$ for the dominant modes of a (neutral) spin-1/2 field in Kerr-dS ($Q = 0$) as a function of a/a_{\max} for $\Lambda M^2 = 0.001$. The mode family and (ℓ, m) values are indicated in the inset. Cf. Fig.2 (top left) in [56].

Appendix C: Equatorial circular photon orbits

Here we give explicit analytic expressions for the angular velocity and the Lyapunov exponent of the equatorial circular photon orbits in KNdS. These quantities yield the QNM frequencies for the PS family in Eq. (9).

Denote by r_{ph}^{\pm} the radii of the (prograde and retrograde) equatorial circular photon orbits with $r_+ \leq r_{\text{ph}}^+ \leq r_{\text{ph}}^-$. The angular velocities of these orbits are then given by $\Omega_{\text{ph}}^{\pm} = 1/b_{\text{ph}}^{\pm}$, where

$$b_{\text{ph}}^{\pm} \equiv a \frac{a^2 (r_{\text{ph}}^{\pm})^2 + L^2 (r_{\text{ph}}^{\pm} (3M + r_{\text{ph}}^{\pm}) - 2Q^2)}{a^2 (r_{\text{ph}}^{\pm})^2 - L^2 (r_{\text{ph}}^{\pm} (r_{\text{ph}}^{\pm} - 3M) + 2Q^2)}. \quad (\text{C1})$$

Analyzing null geodesics resulting from perturbations away from these orbits, $r = r_{\text{ph}}^{\pm} + \delta r^{\pm}$, we obtain $\delta r^{\pm} = \exp(\lambda^{\pm} t)$ where

$$\lambda^{\pm} = \left| \sqrt{\frac{3Mr_{\text{ph}}^{\pm} - 4Q^2}{Mr_{\text{ph}}^{\pm} - Q^2} \frac{\beta_{\text{ph}}^{\pm} \left[a^2 - a b_{\text{ph}}^{\pm} + (r_{\text{ph}}^{\pm})^2 \right]}{\Xi b_{\text{ph}}^{\pm} r_{\text{ph}}^{\pm} (b_{\text{ph}}^{\pm} - a)}} \right| \quad (\text{C2})$$

are the associated Lyapunov exponents, such that $\lambda^+ \leq \lambda^-$, and

$$\beta_{\text{ph}}^{\pm} \equiv \sqrt{1 + \frac{(a - b_{\text{ph}}^{\pm})^2}{L^2}}.$$

In order to reduce index cluttering, it is $\lambda \equiv \lambda^+$, $\Omega_{\text{ph}} \equiv \Omega_{\text{ph}}^+$ and $r_{\text{ph}} \equiv r_{\text{ph}}^+$ in the main text.

-
- [1] R. Penrose, in *General Relativity: An Einstein centenary survey*, edited by S. W. Hawking and W. Israel (1979) pp. 581–638.
- [2] D. Christodoulou, in *On recent developments in theoretical and experimental general relativity, astrophysics and relativistic field theories. Proceedings, 12th Marcel Grossmann Meeting on General Relativity, Paris, France, July 12-18, 2009. Vol. 1-3* (2008) pp. 24–34, arXiv:0805.3880 [gr-qc].
- [3] E. Poisson and W. Israel, Phys. Rev. Lett. **63**, 1663 (1989).
- [4] A. Ori, Phys. Rev. Lett. **67**, 789 (1991).
- [5] M. Dafermos, Commun. Pure Appl. Math. **58**, 445 (2005).
- [6] J. Luk and S.-J. Oh, arXiv:1702.05715 (2017).
- [7] J. Luk and S.-J. Oh, Duke Math. J. **166**, 437 (2017).
- [8] A. Ori, Phys. Rev. Lett. **68**, 2117 (1992).
- [9] M. Dafermos and J. Luk, arXiv:1710.01722 (2017).
- [10] M. Dafermos and Y. Shlapentokh-Rothman, Commun. Math. Phys. **350**, 985 (2017), arXiv:1512.08260 [gr-qc].
- [11] K. D. Kokkotas and B. G. Schmidt, Living Rev. Relativity **2**, 2 (1999).
- [12] E. Berti, V. Cardoso, and A. O. Starinets, Class. Quant. Grav. **26**, 163001 (2009), arXiv:0905.2975 [gr-qc].
- [13] P. Hintz and A. Vasy, J. Math. Phys. **58**, 081509 (2017), arXiv:1512.08004 [math.AP].
- [14] O. J. C. Dias, F. C. Eperon, H. S. Reall, and J. E. Santos, Phys. Rev. D **97**, 104060 (2018).
- [15] O. J. C. Dias, H. S. Reall, and J. E. Santos, J. High Energy Phys. **2018**, 1 (2018).
- [16] K. Destounis, Physics Letters B **795**, 211219 (2019).
- [17] V. Cardoso, J. a. L. Costa, K. Destounis, P. Hintz, and A. Jansen, Phys. Rev. D **98**, 104007 (2018).
- [18] B. Ge, J. Jiang, B. Wang, H. Zhang, and Z. Zhong, J. High Energy Phys. **2019** (2019).
- [19] X. Liu, S. Van Vooren, H. Zhang, and Z. Zhong, J. High Energy Phys. **2019**, 186 (2019), arXiv:1909.07904 [hep-th].
- [20] P. Hintz and A. Vasy, Acta Math. **220**, 1 (2018).
- [21] P. Hintz, Annals of PDE **4**, 1 (2016).
- [22] J. L. Costa, P. M. Girão, J. Natário, and J. D. Silva, Commun. Math. Phys. **361**, 289 (2018).
- [23] R. Luna, M. Zilhão, V. Cardoso, J. L. Costa, and J. Natário, Phys. Rev. D **99**, 064014 (2019).
- [24] V. Cardoso, J. L. Costa, K. Destounis, P. Hintz, and A. Jansen, Phys. Rev. Lett. **120**, 031103 (2018), arXiv:1711.10502 [gr-qc].
- [25] Y. Mo, Y. Tian, B. Wang, H. Zhang, and Z. Zhong, Phys. Rev. D **98**, 124025 (2018).
- [26] O. J. C. Dias, H. S. Reall, and J. E. Santos, Class. Quant. Grav. **36**, 045005 (2019), arXiv:1808.04832 [gr-qc].
- [27] H. Guo, H. Liu, X.-M. Kuang, and B. Wang, Eur. Phys. J. C **79**, 891 (2019), arXiv:1905.09461 [gr-qc].
- [28] S. Hod, Nucl. Phys. B **941**, 636 (2019).
- [29] H. Zhang and Z. Zhong, arXiv:1910.01610 (2019).
- [30] C. F. Gammie, S. L. Shapiro, and J. C. McKinney, Astrophys. J. **602**, 312 (2004).
- [31] S. Hod, Physics Letters B **780**, 221 (2018).
- [32] M. Rahman, S. Chakraborty, S. SenGupta, and A. A. Sen, JHEP **03**, 178 (2019), arXiv:1811.08538 [gr-qc].
- [33] B. Carter, Commun. Math. Phys. (1965-1997) **10**, 280 (1968).
- [34] G. Gibbons and S. Hawking, Phys. Rev. **D15**, 2738 (1977).
- [35] H. Suzuki, E. Takasugi, and H. Umetsu, Prog. Theor. Phys. **100**, 491 (1998).
- [36] C. J. Goebel, Astrophys. J. **172**, L95+ (1972).
- [37] B. Mashhoon, Phys. Rev. D **31**, 290 (1985).
- [38] V. Cardoso, A. S. Miranda, E. Berti, H. Witek, and V. T. Zanchin, Phys. Rev. D **79**, 064016 (2009), arXiv:0812.1806 [hep-th].
- [39] S. R. Dolan, Phys. Rev. **D82**, 104003 (2010), arXiv:1007.5097 [gr-qc].
- [40] H. Yang, D. A. Nichols, F. Zhang, A. Zimmerman, Z. Zhang, and Y. Chen, Phys. Rev. **D86**, 104006 (2012), arXiv:1207.4253 [gr-qc].
- [41] M. Casals and C. I. Marinho, In preparation.
- [42] H. Yang, A. Zimmerman, A. Zenginoğlu, F. Zhang, E. Berti, and Y. Chen, Phys. Rev. D **88**, 044047 (2013).
- [43] S. Hod, Eur. Phys. J. **C77**, 351 (2017), arXiv:1705.04726 [hep-th].
- [44] S. Detweiler, Astrophys. J. **239**, 292 (1980).
- [45] A. Lopez-Ortega, Gen. Rel. Grav. **38**, 743 (2006), arXiv:gr-qc/0605022 [gr-qc].
- [46] M. Casals and A. C. Ottewill, Phys. Rev. **D71**, 064025 (2005), arXiv:gr-qc/0409012.

- [47] S. Perlmutter *et al.* (Supernova Cosmology Project), *Astrophys. J.* **517**, 565 (1999), arXiv:astro-ph/9812133 .
- [48] A. G. Riess *et al.*, *Astron. J.* **116**, 1009 (1998), arXiv:astro-ph/9805201 [astro-ph] .
- [49] R. D. Blandford and R. L. Znajek, *Mon. Not. R. Astron. Soc.* **179**, 433 (1977).
- [50] M. Dafermos and Y. Shlapentokh-Rothman, *Class. Quant. Grav.* **35**, 195010 (2018), arXiv:1805.08764 [gr-qc] .
- [51] S. Hollands, R. M. Wald, and J. Zahn, *Class. Quantum Gravity* **37**, 115009 (2020).
- [52] E. W. Leaver, *Proc. Roy. Soc. Lond. A* **402**, 285 (1985).
- [53] S. Yoshida, N. Uchikata, and T. Futamase, *Phys. Rev. D* **81**, 044005 (2010).
- [54] J.-F. Chang and Y.-G. Shen, *Nucl. Phys. B* **712**, 347 (2005).
- [55] R. A. Konoplya and A. Zhidenko, *Phys. Rev. D* **76**, 084018 (2007), [Erratum: *Phys. Rev. D* **90**, no.2, 029901(2014)], arXiv:0707.1890 [hep-th] .
- [56] R. Mostafizur, *Eur. Phys. J. C, Particles and Fields.* **80** (2020).
- [57] K. Destounis, R. D. B. Fontana, and F. C. Mena, “Counterexamples to strong cosmic censorship in asymptotically flat black hole spacetimes,” (2020), arXiv:2006.01152 [gr-qc] .
- [58] Z. Zhu, S.-J. Zhang, C. Pellicer, B. Wang, and E. Abdalla, *Phys. Rev. D* **90**, 044042 (2014).
- [59] F. Novaes, C. I. Marinho, M. Lencsés, and M. Casals, *JHEP* **05**, 033 (2019), arXiv:1811.11912 [gr-qc] .
- [60] In the case of an *accelerated*, asymptotically flat and charged but non-rotating (C-metric) black hole, it has recently been shown in [57] that SCC may be violated.
- [61] In fact, in a certain region of parameter space for a charged and minimally-coupled scalar field, Refs. [17, 25, 26] find frequencies with a *positive* imaginary part, corresponding to an instability of the *exterior* of the black hole, as originally seen in [58] in the massless case. Ref. [27] found that such instability is present for a massless neutral scalar field in RNdS as long as the coupling constant is negative. For a massless *conformally*-coupled charged scalar field and a charged Dirac field in KNdS, which are the cases we consider, no such exterior instability seems to exist [55] .
- [62] We note that, because of the so-called Teukolsky-Starobinsky identities [35], the QNM frequencies for $s = 1/2$ are the same as for $s = -1/2$.
- [63] Unfortunately, the decoupling of the equations for electromagnetic ($|s| = 1$) and gravitational perturbations ($|s| = 2$) has not yet been achieved.
- [64] Reassuringly, it is easy to check that, replacing r_- by r_c and $-m\bar{\Omega}$ by $m\bar{\Omega} + q\bar{\phi}$ in Eq. (4.16) of Ref. [59], which was obtained for neutral fields in the $r_c \rightarrow r_+$ limit of Kerr-dS satisfying the appropriate QNM boundary conditions at both $r \rightarrow r_{+,c}$, the result agrees with our Eq. (10). In fact, we checked that, when including the higher order term in Eq. (4.18) of [59] and applying the mentioned replacements, the resulting asymptotics agree with our numerical results to even higher precision. Furthermore, Eq. (10) is invariant under $s \rightarrow -s$, as expected.
- [65] It so happens that, at extremality, $r_{\text{ph}} = r_+$ if $a \gtrsim \bar{a}$ whereas $r_{\text{ph}} > r_+$ if $a \lesssim \bar{a}$, given some values of M , Λ and Q . We also note that, at extremality, \bar{a}/r_+ is equal to the critical value \bar{a}_c^{KNdS} in [31].
- [66] We have further checked that, as Q approaches Q_{max} , the amplitude of the wiggles, as gathered from Fig.3, does not decrease faster than $1/2 - \beta_+$
- [67] Similar wiggles in RNdS were already noticed in Refs. [16, 26] for near-maximal charge and are related to similar wiggles in Kerr for near-maximal rotation [42].